crystals

MDPI

Opinion

Sulfur Line Vacancies in MoS_2 for Catalytic Hydrogen Evolution Reaction

Meng Tang, Weinan Yin, Shijie Liu, Haoxuan Yu, Yuhao He, Yuntao Cai and Longlu Wang *

College of Electronic and Optical Engineering & College of Flexible Electronics (Future Technology), Nanjing University of Posts and Telecommunications, Nanjing 210023, China
* Correspondence: wanglonglu@njupt.edu.cn

Abstract: Defects in transition metal dichalcogenides play important roles in the field of the catalytic hydrogen evolution reaction (HER). However, the use of defective MoS_2 as HER catalysts remains controversial because the types of defects are various, including zero-dimensional point defects, one-dimensional linear defects, and two-dimensional plane defects. Recently, novel structures of linear defects have drawn more and more attention, and it is necessary to explore their unique properties. This review focuses on the formation mechanism, fabrication method, accurate atomic structure, and catalytic hydrogen evolution mechanism of sulfur line vacancies in MoS_2 as electrocatalysts. The structure–activity relationship between line defects and catalytic performance is discussed in detail. This will provide a route for the design of excellent catalysts by engineering line defects.

Keywords: sulfur line vacancies in MoS_2; atomic structure; MoS_2; hydrogen evolution reaction

Citation: Tang, M.; Yin, W.; Liu, S.; Yu, H.; He, Y.; Cai, Y.; Wang, L. Sulfur Line Vacancies in MoS_2 for Catalytic Hydrogen Evolution Reaction. *Crystals* **2022**, *12*, 1218. https://doi.org/10.3390/cryst12091218

Academic Editors: Mohammed Rafi Shaik, Syed Farooq Adil and Mujeeb Khan

Received: 9 August 2022
Accepted: 25 August 2022
Published: 29 August 2022

1. Introduction

The development and utilization of new energy is the key to realizing the double carbon strategy, the core of which is the design and preparation of catalytic materials with high performance [1–5]. Hydrogen energy, as a form of high-efficiency, zero-emission, and renewable clean energy, is a new option for optimizing the energy structure and ensuring the national energy supply, and the electrocatalyst is the core of hydrogen for hydrogen production in our country [6–8]. The unique structural features give two-dimensional materials excellent physical and chemical properties and rich scientific connotations.

There are various defect types in monolayer MoS_2, including point defects (vacancy and substitution), dislocation and grain boundaries, etc. [9–15]. These defects will change the electrical properties of monolayer MoS_2 and may induce novel physical phenomena, such as ferromagnetism. However, in practical applications, the existence of defects will lead to the electrical performance of single-layer MoS_2 (reduced mobility, etc.), and the co-existence of different types of defects may make single-layer MoS_2 become a compensation semiconductor [16–20]. Therefore, it is of great significance to accurately identify the different defect types of single-layer MoS_2, control the defect concentration, and then regulate the band structure and electrical properties of single-layer MoS_2 for relevant application research. Chalcogen vacancy lines, another frequently observed 1D line defect in 2D TMD materials, can provide additional metallic channels and thus promote catalytic performance, such as the hydrogen evolution reaction (HER) activity of the host materials [21–27].

Sulfur line vacancy engineering triggered by an electron beam (e-beam), plasma, chemical treatment, and so forth is comprehensively reviewed. Firstly, e-beam irradiation-induced defect evolution, structural transformation, and novel structure fabrication are introduced [28–34]. With the assistance of state-of-the-art characterization methods, in situ observation of sulfur line vacancy engineering could be realized. Thus, the catalytic HER mechanism of MoS_2 could be ascertained. The challenges and outlooks of sulfur line vacancy engineering in promoting the development of 2D materials are discussed. Through this review, we aim to build a correlation between the sulfur line vacancies and

HER catalytic properties of 2D materials to support the design and enhancement of high catalytic HER performance.

2. Understanding Linear Defects

Understanding the atomic structure and dynamic evolution of defects is of great significance for the improvement and performance of two-dimensional material functional devices [35–38]. Spherical aberration correction transmission electron microscopy not only has subangstrom spatial resolution but also has many experimental functions [35–40]. It is a very effective method for studying the structure–activity relationship of materials by simultaneously studying the crystal structure of materials and the corresponding electronic structure characteristics at the atomic scale so as to understand the correlation between the microscopic crystal structure and the properties of samples. Therefore, it has a very wide range of applications in physics, materials science, and chemistry.

The defect structures of two-dimensional materials are closely related to their physical and chemical properties, but systematic research on them is still relatively rare. To date, high-resolution images of monolayer MoS_2 have been obtained using high-resolution scanning transmission electron microscopy (STEM) to identify defect types such as vacancies, substitutions, and grain boundaries [40–46]. However, in order to achieve STEM representation, MoS_2 needs to be transferred from the growing substrate to the STEM microgate for imaging, and high-energy electron beam bombardment will also induce the generation of defects. In contrast, scanning tunneling microscopy/tunneling spectroscopy (STM/STS) in an ultra-high vacuum system can not only realize the in situ atomic-scale morphology study but also clarify the evolution of electronic structures induced by different defect types, which provides the most intuitive experimental basis for the subsequent application research of materials [47–54]. Based on this, Liu et al. reported the generation mechanism of different types of sulfur vacancies in monolayer MoS_2 and studied the regulation effect of different defect types on the band structure of monolayer MoS_2 by STM/STS technology. It was found that with the increase in the sample annealing temperature (400 to 900 K), the density of S vacancies gradually increases, and S vacancies will aggregate to form a chain structure (S2, S3, S4, etc.) [43]. The STS measurements show that the formation of S vacancies induces the formation of new electronic states at the bottom of the conduction band and leads to a smaller band gap (2.2 eV after annealing at 400 K; 1.8 eV after annealing at 900 K), and an N-type doping effect on monolayer MoS_2 is produced. Combined with data statistics and theoretical calculations, it was found that the chemical potential of S in single S vacancy and chain S vacancy structures is almost the same (−6.87 eV~−6.5 eV), indicating that the concentration of different types of defects strictly complies with the thermodynamic statistical law, and temperature is the only inducing factor for the formation of defects. This work provides the most intuitive experimental basis and theoretical analysis for understanding the generation and regulation mechanism of defects in monolayer MoS_2, as well as its regulatory effect on the local electronic structure, and also provides a reference for the future application of semiconducting monolayer disulfide compounds in electronic devices. An atomic model of the 1D vacancy line consisting of 2S missing atomic rows is shown in Figure 1a. This type of 1D line defect in MoS_2 and WS_2 was well studied by 4D STEM, as reported by Warner et al. Electron beam irradiation can create defects in 2D materials due to either a "knock-on" effect, ionization, or beam-induced chemical etching, facilitating the sculpting of 2D membranes with high spatial accuracy and flexible pattern design. The removal of a single S atom causes little perturbation to the surrounding MoS_2 lattice, while the loss of two S atoms from the same atomic column results in measurable local shrinkage. S vacancies aggregate into linear line defects along a zigzag path, leading to greater lattice compression, which is more pronounced with increasing line defect length. Figure 1b,c show two different types of S atom reconstructions with different amounts of lattice compression. AC-TEM images in Figure 1d,e clearly show the aggregation of S vacancies into extended line defects along a zigzag path with different lengths and widths. The directional transport of Mo atoms (or Mo cluster) along the sulfur

vacancy lines can induce the formation of Mo chains, as shown in Figure 1f. Tarak K. Patra et al. comprehensively studied the dynamic behavior and spatial distribution of defects in 2D transition metal disulfide using machine learning, molecular dynamics simulation, and high-resolution electron microscopy, as shown in Figure 1h. This study provides a good basis for the subsequent rational design and large-scale application of 2D transition metal disulfide-containing defects.

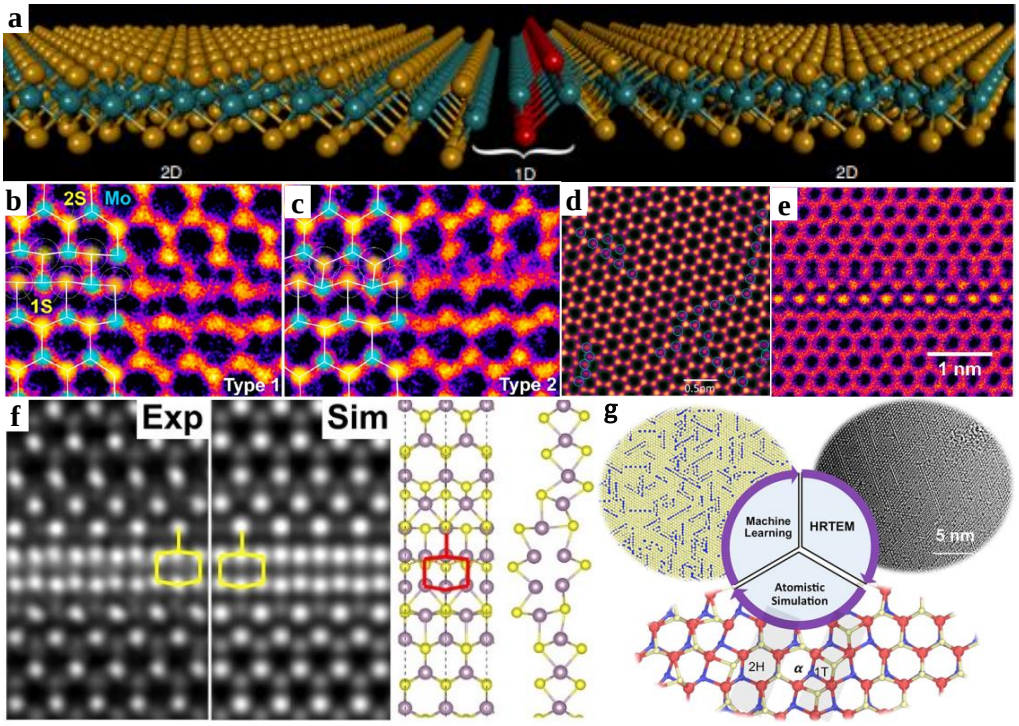

Figure 1. (**a**) Perspective view of an atomic model of the 1D vacancy line consisting of 2S missing atomic rows. (**a**) Adapted with permission from [7]. Copyright Springer Nature 2011. (**b**,**c**) Two different types of S atom reconstructions with different amounts of lattice compression. (**b**,**c**) Adapted with permission from [12]. Copyright 2014 American Chemical Society. (**d**) AC-TEM image showing the aggregation of S vacancies into extended line defects along a zigzag path with different lengths and widths. (**e**) Higher-magnification AC-TEM images at 800 °C of an ultralong line defect in MoS_2 showing uniform atomic periodicity. (**d**,**e**) Adapted with permission from [13]. Copyright 2018 American Chemical Society. (**f**) Experimental (Exp.) and simulated (Sim.) images of the Mo chain in MoS_2 and the corresponding atomic model. (**f**) Adapted with permission from [13]. Copyright 2018 American Chemical Society. (**g**) Defect dynamics in 2-D MoS_2 probed by using machine learning, atomistic simulations, and high-resolution microscopy. (**g**) Adapted with permission from [16]. Copyright 2018 American Chemical Society.

3. Application of Linear Defects for Catalytic HER

As a typical 2D transition metal disulfide compound, the MoS_2 edge structure has moderate hydrogen adsorption strength and exhibits good HER activity [55–62]. Therefore, molybdenum disulfide is widely considered a potential non-precious metal HER catalyst to replace precious metal Pt. However, a large number of sulfur atoms on the molybdenum disulfide surface are inert to electrocatalytic hydrogen evolution, and the number of active edge sites is very limited [63–70]. Therefore, it is of great significance to develop effective methods to stimulate and optimize the S activity on the molybdenum sulfide surface to increase the number of catalytic active sites of MoS_2 and improve its catalytic HER activity [71–76]. The one-dimensional monoatomic molybdenum chain was successfully prepared by regulating the MoS_2 electrocatalyst with sodium ions. The S atoms on the substrate were eliminated linearly. The one-dimensional monoatomic molybdenum chain has a large potential gradient, which makes it easy to accumulate electrons here, storing

them like a "reservoir", and has a higher hydrogen atom coverage, as shown in Figure 2a, which makes catalytic hydrogen evolution easier to proceed. As shown in Figure 2b, multilayer MoS_2 samples rich in sulfur vacancies were prepared by high-temperature hydrogen etching technology, and the role and effect of surface sulfur vacancies on HER catalytic performance were analyzed in detail. Multilayer MoS_2 samples with an ultra-high concentration (90%) of surface sulfur vacancies were prepared to achieve the highest HER activity under alkaline conditions (Figure 2c,d), and their stability could be maintained.

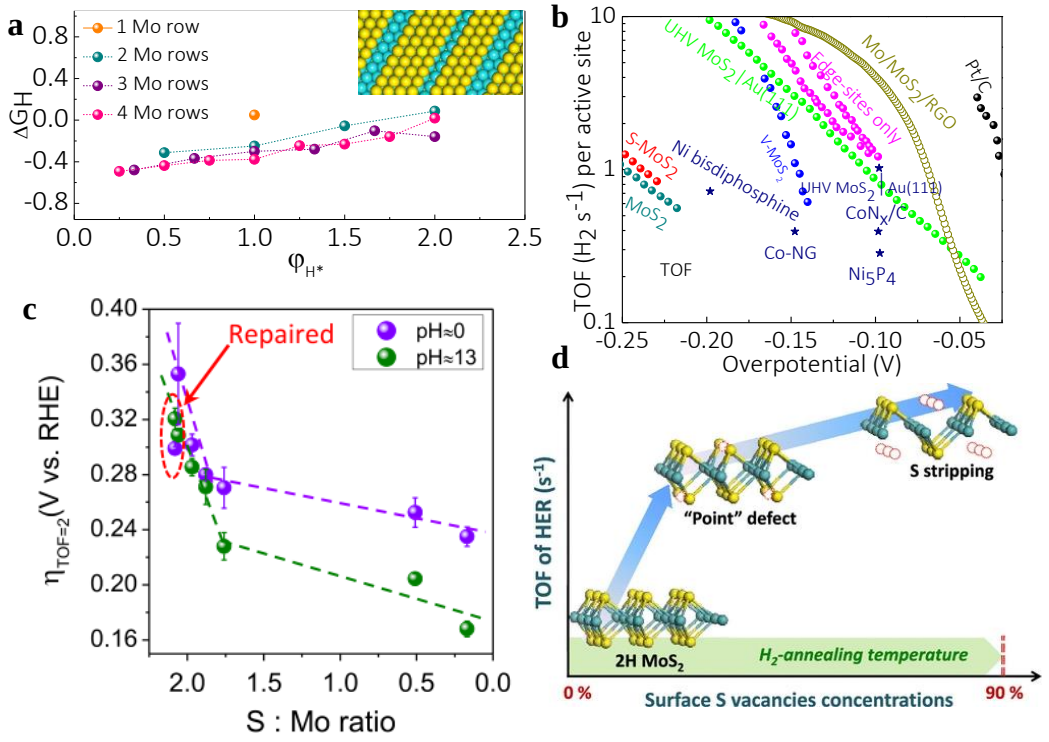

Figure 2. (**a**) Gibbs free energy (ΔG_H) versus hydrogen coverage (ϕH) for MoS_2 with different rows of S chains. The insert is the atomic structure depicting linear defects created by successive removal of S atoms along a row. (**b**) Calculated turnover frequency (TOF) of recently reported MoS_2-based HER electrocatalysts [19]. (**a**,**b**) Adapted with permission from [19]. Copyright 2019 Elsevier. (**c**) Turnover frequency (TOF) from defective MoS_2 nanosheets. (**d**) The influence of controlled surface S vacancies of MoS_2 on their performance toward hydrogen production [14]. (**c**,**d**) Adapted with permission from [14]. Copyright 2019 American Chemical Society.

4. Conclusions and Outlook

In summary, we have witnessed the rapid development of sulfur line vacancies in MoS_2 in terms of both their fabrication strategies and application fields in electrochemical hydrogen evolution. Firstly, although many advanced methods have been proven to be a powerful way of preparing sulfur line vacancies, the development of novel synthesis strategies for the "precise control" of sulfur line vacancies is still challenging but highly required. Secondly, sulfur line vacancies provide a suitable platform for investigating the structure–activity relationships and the potential catalytic mechanisms of hydrogen evolution reactions. Thirdly, theoretical prediction based on computational modeling has proved to be a useful tool for discovering sulfur line vacancies for hydrogen evolution reactions. Strategies based on DFT studies for the rational design of model defects with a precise atomic structure are still highly desired [77–81].

In conclusion, despite the exciting progress achieved in defects for electrochemical energy conversion, both opportunities and challenges remain. Thus, defects with a well-controlled coordination environment and electronic state, combined with advanced in situ/operando techniques and DFT theoretical studies, will pave the way for both funda-

mental research and future industrial applications of sulfur line vacancies for various fields related to electrochemical energy conversion.

(1) The development of in situ dynamic characterization technology and real-time monitoring of the catalytic reaction process is of great significance for the in-depth understanding of reaction mechanisms and the design of efficient catalysts. In situ characterization instruments, especially under operational conditions, can realize the study of the structure and chemical composition of materials under working conditions to a certain extent, which is conducive to understanding the causes of the observed phenomena. Therefore, it is very important and necessary to develop working conditions, sample surface structure, and chemical properties in a growing environment.

(2) The wide application of DFT has produced a large amount of data, but the reliability and intrinsic self-consistency of these data still need extensive attention. In addition, in recent years, research on accelerating traditional quantum chemical computation based on database and machine learning has rapidly emerged, but there is still a lack of original innovation in the underlying methods (neural networks, etc.), and it is urgent to develop "intelligent" tools that can be used for "intelligent" mining catalytic theory and real theoretical research.

Author Contributions: All authors have contributed to the writing of this manuscript. All authors have read and agreed to the published version of the manuscript.

Funding: This work was financially supported by the Natural Science Foundation of China (51902101), the Youth Natural Science Foundation of Hunan Province (2021JJ540044), the Natural Science Foundation of Jiangsu Province (BK20201381), and the Science Foundation of Nanjing University of Posts and Telecommunications (NY219144).

Institutional Review Board Statement: Not applicable.

Informed Consent Statement: Not applicable.

Data Availability Statement: Not applicable.

Conflicts of Interest: The authors declare no conflict of interest.

References

1. Chhowalla, M.; Shin, H.S.; Eda, G.; Li, L.-J.; Loh, K.P.; Zhang, H. The chemistry of two-dimensional layered transition metal dichalcogenide nanosheets. *Nat. Chem.* **2013**, *5*, 263.
2. Wang, Q.H.; Kalantar-Zadeh, K.; Kis, A.; Coleman, J.N.; Strano, M.S. Electronics and optoelectronics of two-dimensional transition metal dichalcogenides. *Nat. Nanotechnol.* **2012**, *7*, 699–712. [PubMed]
3. Manzeli, S.; Dumcenco, D.; Migliato Marega, G.; Kis, A. Self-Sensing, Tunable Monolayer MoS_2 Nanoelectromechanical Resonators. *Nat. Commun.* **2019**, *10*, 4831. [PubMed]
4. Siao, M.D.; Shen, W.C.; Chen, R.S.; Chang, Z.W.; Shih, M.C.; Chiu, Y.P.; Cheng, C.-M. Two-Dimensional Electronic Transport and Surface Electron Accumulation in MoS_2. *Nat. Commun.* **2018**, *9*, 1442. [PubMed]
5. Johari, P.; Shenoy, V.B. Tuning the Electronic Properties of Semiconducting Transition Metal Dichalcogenides by Applying Mechanical Strains. *ACS Nano* **2012**, *6*, 5449–5456.
6. Fiori, G.; Bonaccorso, F.; Iannaccone, G.; Palacios, T.; Neumaier, D.; Seabaugh, A.; Banerjee, S.K.; Colombo, L. Electronics based on two-dimensional materials. *Nat. Nanotechnol.* **2014**, *9*, 768.
7. Fang, S.; Wen, Y.; Allen, C.S.; Ophus, C.; Han, G.G.D.; Kirkland, A.I.; Kaxiras, E.; Warner, J.H. Atomic electrostatic maps of 1D channels in 2D semiconductors using 4D scanning transmission electron microscopy. *Nat. Commun.* **2019**, *10*, 1127. [CrossRef]
8. Jiao, Y.; Hafez, A.M.; Cao, D.; Mukhopadhyay, A.; Ma, Y.; Zhu, H. Metallic MoS_2 for High Performance Energy Storage and Energy Conversion. *Small* **2018**, *14*, 1800640.
9. Guguchia, Z.; Kerelsky, A.; Edelberg, D.; Banerjee, S.; von Rohr, F.; Scullion, D.; Augustin, M.; Scully, M.; Rhodes, D.A.; Shermadini, Z.; et al. Magnetism in Semiconducting Molybdenum Dichalcogenides. *Sci. Adv.* **2018**, *4*, 12.
10. Liang, S. Electrical Spin Injection and Detection in Molybdenum Disulfide Multilayer Channel. *Nat. Commun.* **2019**, *8*, 9.
11. Garcia-Esparza, A.T.; Park, S.; Abroshan, H.; Mellone, O.A.P.; Vinson, J.; Abraham, B.; Kim, T.R.; Nordlud, D.; Gallo, A.; Alonso-Mori, R.; et al. Local Structure of Sulfur Vacancies on the Basal Plane of Monolayer MoS_2. *ACS Nano* **2022**, *16*, 6725–6733. [CrossRef] [PubMed]
12. Wang, S.; Lee, G.D.; Lee, S.; Yoon, E.; Warner, J.H. Detailed atomic reconstruction of extended line defects in monolayer MoS_2. *ACS Nano* **2016**, *10*, 5419–5430. [CrossRef] [PubMed]

13. Chen, Q.; Li, H.; Zhou, S.; Xu, W.; Chen, J.; Sawada, H.; Allen, C.S.; Kirkland, A.I.; Grossman, J.C.; Warner, J.H. Ultralong 1D vacancy channels for rapid atomic migration during 2D void formation in monolayer MoS_2. *ACS Nano* **2018**, *12*, 7721–7730. [CrossRef]
14. Li, L.; Qin, Z.; Ries, L.; Hong, S.; Michel, T.; Yang, J.; Salameh, C.; Bechelany, M.; Miele, P.; Kaplan, D.; et al. Role of sulfur vacancies and undercoordinated Mo regions in MoS_2 nanosheets toward the evolution of hydrogen. *ACS Nano* **2019**, *13*, 6824–6834. [CrossRef]
15. Zhou, S.; Wang, S.; Li, H.; Xu, W.; Gong, C.; Grossman, J.C.; Warner, J.H. Atomic structure and dynamics of defects in 2D MoS_2 bilayers. *ACS Omega* **2017**, *2*, 3315–3324. [CrossRef]
16. Patra, T.K.; Zhang, F.; Schulman, D.S.; Chan, H.; Cherukara, M.J.; Terrones, M.; Das, S.; Narayanan, B.; Sankaranarayanan, S.K.R.S. Defect Dynamics in 2-D MoS_2 Probed by Using Machine Learning, Atomistic Simulations, and High-Resolution Microscopy. *ACS Nano* **2018**, *12*, 8006–8016.
17. Jariwala, D.; Sangwan, V.K.; Lauhon, L.J.; Marks, T.J.; Hersam, M.C. Emerging Device Applications for Semiconducting Two-Dimensional Transition Metal Dichalcogenides. *ACS Nano* **2014**, *8*, 1102–1120. [PubMed]
18. Wang, X.; Wang, X.; Huang, J.; Li, S.; Meng, A.; Li, Z. Interfacial chemical bond and internal electric field modulated Z-scheme Sv-$ZnIn_2S_4$/$MoSe_2$ photocatalyst for efficient hydrogen evolution. *Nat. Commun.* **2021**, *12*, 4112.
19. Wang, L.; Liu, X.; Zhang, Q.; Zhou, G.; Pei, Y.; Chen, S.; Wang, J.; Rao, A.M.; Yang, H.; Lu, B. Quasi-one-dimensional Mo chains for efficient hydrogen evolution reaction. *Nano Energy* **2019**, *61*, 194–200.
20. Bhimanapati, G.R.; Lin, Z.; Meunier, V.; Jung, Y.; Cha, J.; Das, S.; Xiao, D.; Son, Y.; Strano, M.S.; Cooper, V.R.; et al. Recent Advances in Two-Dimensional Materials beyond Graphene. *ACS Nano* **2015**, *9*, 11509–11539.
21. Tsai, C.; Li, H.; Park, S.; Park, J.; Han, H.S.; Nørskov, J.K.; Zheng, X.; Abild-Pedersen, F. Electrochemical generation of sulfur vacancies in the basal plane of MoS_2 for hydrogen evolution. *Nat. Commun.* **2017**, *8*, 15113. [PubMed]
22. Li, H.; Tsai, C.; Koh, A.L.; Cai, L.; Contryman, A.W.; Fragapane, A.H.; Zhao, J.; Han, H.S.; Manoharan, H.C.; Abild-Pedersen, F.; et al. Activating and optimizing MoS_2 basal planes for hydrogen evolution through the formation of strained sulphur vacancies. *Nat. Mater.* **2016**, *15*, 48–53. [CrossRef] [PubMed]
23. Radisavljevic, B.; Radenovic, A.; Brivio, J.; Giacometti, V.; Kis, A. Single-layer MoS_2 transistors. *Nat. Nanotechnol.* **2011**, *6*, 147–150. [CrossRef]
24. Komsa, H.P.; Kurasch, S.; Lehtinen, O.; Kaiser, U.; Krasheninnikov, A.V. From point to extended defects in two-dimensional MoS_2: Evolution of atomic structure under electron irradiation. *Phys. Rev. B* **2013**, *88*, 035301.
25. Xu, S.G.; He, C.C.; Zhao, Y.J.; Xu, H.; Yang, X.B. Unconventional line defects engineering in two-dimensional boron monolayers. *Phys. Rev. Mater.* **2021**, *5*, 044003.
26. Wang, X.W.; Hou, L.F.; Huang, W.; Ren, X.B.; Ji, W.; Jin, C.H. Mass transport induced structural evolution and healing of sulfur vacancy lines and Mo chain in monolayer MoS_2. *Rare Met.* **2022**, *41*, 333–341.
27. Ganatra, R.; Zhang, Q. Few-Layer MoS_2: A Promising Layered Semiconductor. *ACS Nano* **2014**, *8*, 4074–4099.
28. Tai, K.L.; Huang, C.W.; Cai, R.F.; Huang, G.M.; Tseng, Y.T.; Chen, J.; Wu, W.W. Atomic-scale fabrication of in-plane heterojunctions of few-layer MoS_2 via in situ scanning transmission electron microscopy. *Small* **2020**, *16*, 1905516. [CrossRef]
29. Ryu, G.H.; Lee, J.; Kim, N.Y.; Lee, Y.; Kim, Y.; Kim, M.J. Line-defect mediated formation of hole and Mo clusters in monolayer molybdenum disulfide. *2D Mater.* **2016**, *3*, 014002. [CrossRef]
30. Man, P.; Srolovitz, D.; Zhao, J.; Ly, T.H. Functional grain boundaries in two-dimensional transition-metal dichalcogenides. *Acc. Chem. Res.* **2021**, *54*, 4191–4202. [CrossRef]
31. Calderon, V.S.; Ferreira, R.V.; Taneja, D.; Jayanth, R.T.; Zhou, L.; Ribeiro, R.M.; Akinwande, D.; Ferreira, P.J. Atomic Electrostatic Maps of Point Defects in MoS_2. *Nano Lett.* **2021**, *21*, 10157–10164. [CrossRef]
32. Zhu, Y.; Tao, L.; Chen, X.; Ma, Y.; Ning, S.; Zhou, J.; Zhao, X.; Bosman, M.; Liu, Z.; Du, S.; et al. Anisotropic point defects in rhenium diselenide monolayers. *iScience* **2021**, *24*, 103456.
33. Kang, S.; Koo, J.J.; Seo, H.; Truong, Q.T.; Park, J.B.; Park, S.C.; Jung, Y.; Cho, S.P.; Nam, K.T.; Kim, Z.H.; et al. Defect-engineered MoS_2 with extended photoluminescence lifetime for high-performance hydrogen evolution. *J. Mater. Chem. C* **2019**, *7*, 10173–10178. [CrossRef]
34. Guo, S.; Fu, J.; Zhang, P.; Zhu, C.; Yao, H.; Xu, M.; An, B.; Wang, X.; Tang, B.; Deng, Y.; et al. Direct growth of single-metal-atom chains. *Nat. Synth.* **2022**, *1*, 245–253. [CrossRef]
35. Qorbani, M.; Sabbah, A.; Lai, Y.R.; Kholimatussadiah, S.; Quadir, S.; Huang, C.Y.; Shown, I.; Huang, Y.F.; Hayashi, M.; Chen, L.C.; et al. Atomistic insights into highly active reconstructed edges of monolayer 2H-WSe_2 photocatalyst. *Nat. Commun.* **2022**, *13*, 1256.
36. Vancsó, P.; Magda, G.Z.; Pető, J.; Noh, J.Y.; Kim, Y.S.; Hwang, C.; Biró, L.P.; Tapasztó, L. The intrinsic defect structure of exfoliated MoS_2 single layers revealed by Scanning Tunneling Microscopy. *Sci. Rep.* **2016**, *6*, 29726. [CrossRef]
37. Sukanya, R.; da silva Alves, D.C.; Breslin, C.B. Recent Developments in the Applications of 2D Transition Metal Dichalcogenides as Electrocatalysts in the Generation of Hydrogen for Renewable Energy Conversion. *J. Electrochem. Soc.* **2022**, *169*, 064504.
38. Xie, L.; Wang, L.; Zhao, W.; Liu, S.; Huang, W.; Zhao, Q. WS_2 moiré superlattices derived from mechanical flexibility for hydrogen evolution reaction. *Nat. Commun.* **2022**, *12*, 5070. [CrossRef]
39. Wang, L.; Xie, L.; Zhao, W.; Liu, S.; Zhao, Q. Oxygen-facilitated dynamic active-site generation on strained MoS_2 during photo-catalytic hydrogen evolution. *Chem. Eng. J.* **2021**, *405*, 127028.

40. Wang, S.; Wang, L.; Xie, L.; Zhao, W.; Liu, X.; Zhuang, Z.; Zhuang, Y.; Chen, J.; Liu, S.; Zhao, Q. Dislocation-strained MoS_2 nanosheets for high-efficiency hydrogen evolution reaction. *Nano Res.* **2022**, *15*, 4996–5003.
41. Sun, J.; Li, X.; Guo, W.; Zhao, M.; Fan, X.; Dong, Y.; Xu, C.; Deng, J.; Fu, Y. Synthesis Methods of Two-Dimensional MoS_2: A Brief Review. *Crystals* **2017**, *7*, 198. [CrossRef]
42. Park, M.; Park, Y.J.; Chen, X.; Park, Y.-K.; Kim, M.-S.; Ahn, J.-H. MoS_2-Based Tactile Sensor for Electronic Skin Applications. *Adv. Mater.* **2016**, *28*, 2556–2562. [CrossRef]
43. Cheng, X.; Wang, L.; Xie, L.; Sun, C.; Zhao, W.; Liu, X.; Zhuang, Z.; Liu, S.; Zhao, Q. Defect-driven selective oxidation of MoS_2 nanosheets with photothermal effect for Photo-Catalytic hydrogen evolution reaction. *Chem. Eng. J.* **2022**, *439*, 135757. [CrossRef]
44. Lin, Z.; Liu, Y.; Halim, U.; Ding, M.; Liu, Y.; Wang, Y.; Jia, C.; Chen, P.; Duan, X.; Wang, C.; et al. Solution-Processable 2D Semiconductors for High-Performance Large-Area Electronics. *Nature* **2018**, *562*, 254–258.
45. Liu, M.; Li, H.; Liu, S.; Wang, L.; Xie, L.; Zhuang, Z.; Sun, C.; Wang, J.; Tang, M.; Sun, S.; et al. Tailoring activation sites of metastable distorted 1T′-phase MoS_2 by Ni doping for enhanced hydrogen evolution. *Nano Res.* **2022**, *15*, 524–530.
46. Cui, X.; Kong, Z.; Gao, E.; Huang, D.; Hao, Y.; Shen, H.; Di, C.; Xu, Z.; Zheng, J.; Zhu, D. Rolling up Transition Metal Dichalcogenide Nanoscrolls via One Drop of Ethanol. *Nat. Commun.* **2018**, *9*, 1301. [CrossRef]
47. Liu, X.; Hou, Y.; Tang, M.; Wang, L. Atom elimination strategy for MoS_2 nanosheets to enhance photocatalytic hydrogen evolution. *Chin. Chem. Lett.* 2022; *in press*. [CrossRef]
48. Liu, C.; Wang, L.; Tang, Y.; Luo, S.; Liu, Y.; Zhang, S.; Zeng, Y.; Xu, Y. Vertical single or few-layer MoS_2 nanosheets rooting into TiO_2 nanofibers for highly efficient photocatalytic hydrogen evolution. *Appl. Catal. B* **2015**, *164*, 1–9. [CrossRef]
49. Wang, L.; Zhang, Q.; Zhu, J.; Duan, X.; Xu, Z.; Liu, Y.; Yang, H.; Lu, B. Nature of extra capacity in MoS_2 electrodes: Molybdenum atoms accommodate with lithium. *Energy Storage Mater.* **2019**, *16*, 37–45. [CrossRef]
50. Smithe, K.K.H.; English, C.D.; Suryavanshi, S.V.; Pop, E. Intrinsic electrical transport and performance projections of synthetic monolayer MoS_2 devices. *2D Mater.* **2017**, *4*, 011009. [CrossRef]
51. Zhang, S.; Liu, X.; Liu, C.; Luo, S.; Wang, L.; Cai, T.; Zeng, Y.; Yuan, J.; Dong, W.; Pei, Y.; et al. MoS_2 quantum dot growth induced by S vacancies in a $ZnIn_2S_4$ monolayer: Atomic-level heterostructure for photocatalytic hydrogen production. *ACS Nano* **2018**, *12*, 751–758. [CrossRef]
52. Xu, Y.; Cheng, C.; Du, S.; Yang, J.; Yu, B.; Luo, J.; Yin, W.; Li, E.; Dong, S.; Ye, P.; et al. Contacts between Two-and Three-Dimensional Materials: Ohmic, Schottky, and p–n Heterojunctions. *ACS Nano* **2016**, *10*, 4895–4919.
53. Li, Y.; Yin, K.; Wang, L.; Lu, X.; Zhang, Y.; Liu, Y.; Yan, D.; Song, Y.; Luo, S. Engineering MoS_2 nanomesh with holes and lattice defects for highly active hydrogen evolution reaction. *Appl. Catal. B* **2018**, *239*, 537–544. [CrossRef]
54. Zhou, J.; Guo, M.; Wang, L.; Ding, Y.; Zhang, Z.; Tang, Y.; Liu, C.; Luo, S. 1T-MoS_2 nanosheets confined among TiO_2 nanotube arrays for high performance supercapacitor. *Chem. Eng. J.* **2019**, *366*, 163–171. [CrossRef]
55. Zhang, S.; Wang, L.; Liu, C.; Luo, J.; Crittenden, J.; Liu, X.; Cai, T.; Yuan, J.; Pei, Y.; Liu, Y. Photocatalytic wastewater purification with simultaneous hydrogen production using MoS_2 QD-decorated hierarchical assembly of $ZnIn_2S_4$ on reduced graphene oxide photocatalyst. *Water Res.* **2017**, *121*, 11–19.
56. Zhang, W.; Wang, Q.; Chen, Y.; Wang, Z.; Wee, A.T.S. Van der Waals stacked 2D layered materials for optoelectronics. *2D Mater.* **2016**, *3*, 022001. [CrossRef]
57. Li, Y.; Wang, L.; Cai, T.; Zhang, S.; Liu, Y.; Song, Y.; Dong, X.; Hu, L. Glucose-assisted synthesize 1D/2D nearly vertical CdS/MoS_2 heterostructures for efficient photocatalytic hydrogen evolution. *Chem. Eng. J.* **2017**, *321*, 366–374. [CrossRef]
58. Xu, Y.; Wang, L.; Liu, X.; Zhang, S.; Liu, C.; Yan, D.; Zeng, Y.; Pei, Y.; Liu, Y.; Luo, S. Monolayer MoS_2 with S vacancies from interlayer spacing expanded counterparts for highly efficient electrochemical hydrogen production. *J. Mater. Chem. A* **2016**, *4*, 16524–16530. [CrossRef]
59. Withers, F.; Pozo-Zamudio, O.D.; Mishchenko, A.; Rooney, A.P.; Gholinia, A.; Watanabe, K.; Taniguchi, T.; Haigh, S.J.; Geim, A.K.; Tartakovskii, A.I.; et al. Light-emitting diodes by band-structure engineering in van der Waals heterostructures. *Nat. Mater.* **2015**, *14*, 301. [CrossRef]
60. Li, Y.; Wang, L.; Zhang, S.; Dong, X.; Song, Y.; Cai, T.; Liu, Y. Cracked monolayer 1T MoS_2 with abundant active sites for enhanced electrocatalytic hydrogen evolution. *Catal. Sci. Technol.* **2017**, *7*, 718–724. [CrossRef]
61. Jariwala, D.; Marks, T.J.; Hersam, M.C. Mixed-dimensional van der Waals heterostructures. *Nat. Mater.* **2017**, *16*, 170.
62. Wang, L.; Liu, X.; Luo, J.; Duan, X.; Crittenden, J.; Liu, C.; Zhang, S.; Pei, Y.; Zeng, Y.; Duan, X. Self-optimization of the active site of molybdenum disulfide by an irreversible phase transition during photocatalytic hydrogen evolution. *Angew. Chem.* **2017**, *129*, 7718–7722.
63. Zhang, S.; Wang, L.; Zeng, Y.; Xu, Y.; Tang, Y.; Luo, S.; Liu, Y.; Liu, C. CdS-Nanoparticles-Decorated Perpendicular Hybrid of MoS_2 and N-Doped Graphene Nanosheets for Omnidirectional Enhancement of Photocatalytic Hydrogen Evolution. *ChemCatChem* **2016**, *8*, 2557–2564.
64. Dong, H.; Gong, C.; Addou, R.; McDonnell, S.; Azcatl, A.; Qin, X.; Wang, W.; Wang, W.; Hinkle, C.L.; Wallace, R.M. Schottky Barrier Height of Pd/MoS_2 Contact by Large Area Photoemission Spectroscopy. *ACS Appl. Mater. Interfaces* **2017**, *9*, 38977–38983.
65. McDonnell, S.; Addou, R.; Buie, C.; Wallace, R.M.; Hinkle, C.L. Defect-Dominated Doping and Contact Resistance in MoS_2. *ACS Nano* **2014**, *8*, 2880–2888.
66. Sun, C.; Liu, M.; Wang, L.; Xie, L.; Zhao, W.; Li, J.; Liu, S.; Yan, D.; Zhao, Q. Revisiting lithium-storage mechanisms of molybdenum disulfide. *Chin. Chem. Lett.* **2021**, *33*, 1779–1797.

67. Addou, R.; McDonnell, S.; Barrera, D.; Guo, Z.; Azcatl, A.; Wang, J.; Zhu, H.; Hinkle, C.L.; Quevedo-Lopez, M.; Alshareef, H.N.; et al. Impurities and Electronic Property Variations of Natural MoS_2 Crystal Surfaces. *ACS Nano* **2015**, *9*, 9124–9133.
68. Zhang, Q.; Wang, L.; Wang, J.; Yu, X.; Ge, J.; Zhang, H.; Lu, B. Semimetallic vanadium molybdenum sulfide for high-performance battery electrodes. *J. Mater. Chem. A* **2018**, *6*, 9411–9419.
69. Liu, H.; Neal, A.T.; Ye, P.D. Channel Length Scaling of MoS_2 MOSFETs. *ACS Nano* **2012**, *6*, 8563–8569.
70. Wang, L.; Duan, X.; Wang, G.; Liu, C.; Luo, S.; Zhang, S.; Zeng, Y.; Xu, Y.; Liu, Y.; Duan, X. Omnidirectional enhancement of photocatalytic hydrogen evolution over hierarchical "cauline leaf" nanoarchitectures. *Appl. Catal. B* **2016**, *186*, 88–96. [CrossRef]
71. Gao, M.-R.; Chan, M.K.Y.; Sun, Y. Edge-Terminated Molybdenum Disulfide with a 9.4-Å Interlayer Spacing for Electrochemical Hydrogen Production. *Nat. Commun.* **2015**, *6*, 7493. [CrossRef] [PubMed]
72. Chen, J.; Tang, Y.; Wang, S.; Xie, L.; Chang, C.; Cheng, X.; Liu, M.; Wang, L.; Wang, L. Ingeniously designed Ni-Mo-S/$ZnIn_2S_4$ composite for multi-photocatalytic reaction systems. *Chin. Chem. Lett.* **2022**, *33*, 1468–1474. [CrossRef]
73. Zhou, G.; Shan, Y.; Wang, L.; Hu, Y.; Guo, J.; Hu, F.; Shen, J.; Gu, Y.; Cui, J.; Liu, L.; et al. Photoinduced semiconductor-metal transition in ultrathin troilite FeS nanosheets to trigger efficient hydrogen evolution. *Nat. Commun.* **2019**, *10*, 399. [CrossRef]
74. He, Q.; Wang, L.; Yin, K.; Luo, S. Vertically aligned ultrathin 1T-WS_2 nanosheets enhanced the electrocatalytic hydrogen evolution. *Nanoscale Res. Lett.* **2018**, *13*, 167. [CrossRef] [PubMed]
75. Desai, S.B.; Madhvapathy, S.R.; Sachid, A.B.; Llinas, J.P.; Wang, Q.; Ahn, G.H.; Pitner, G.; Kim, M.J.; Bokor, J.; Hu, C.; et al. MoS_2 transistors with 1-nanometer gate lengths. *Science* **2016**, *354*, 99–102. [CrossRef]
76. Zhu, Y.; Chen, J.; Shao, L.; Xia, X.; Liu, Y.; Wang, L. Oriented facet heterojunctions on CdS nanowires with high photoactivity and photostability for water splitting. *Appl. Catal. B* **2020**, *268*, 118744. [CrossRef]
77. Lopez-Sanchez, O.; Lembke, D.; Kayci, M.; Radenovic, A.; Kis, A. Ultrasensitive photodetectors based on monolayer MoS_2. *Nat. Nanotechnol.* **2013**, *8*, 497–501. [CrossRef]
78. Sun, C.; Wang, L.; Zhao, W.; Xie, L.; Wang, J.; Li, J.; Li, B.; Liu, S.; Zhuang, Z.; Zhao, Q. Atomic-Level Design of Active Site on Two-Dimensional MoS_2 toward Efficient Hydrogen Evolution: Experiment, Theory, and Artificial Intelligence Modelling. *Adv. Funct. Mater.* **2022**, 2206163. [CrossRef]
79. Yu, S.H.; Lee, Y.; Jang, S.K.; Kang, J.; Jeon, J.; Lee, C.; Lee, J.Y.; Kim, H.; Hwang, E.; Lee, S.; et al. Dye-Sensitized MoS_2 Photodetector with Enhanced Spectral Photoresponse. *ACS Nano* **2014**, *8*, 8285–8291. [CrossRef]
80. Fazio, D.D.; Goykhman, I.; Yoon, D.; Bruna, M.; Eiden, A.; Milana, S.; Sassi, U.; Barbone, M.; Dumcenco, D.; Marinov, K.; et al. High Responsivity, Large-Area Graphene/MoS_2 Flexible Photodetectors. *ACS Nano* **2016**, *10*, 8252–8262. [CrossRef]
81. Chang, C.; Wang, L.; Xie, L.; Zhao, W.; Liu, S.; Zhuang, Z.; Liu, S.; Li, J.; Liu, X.; Zhao, Q. Amorphous molybdenum sulfide and its Mo-S motifs: Structural characteristics, synthetic strategies, and comprehensive applications. *Nano Res.* **2022**, *15*, 8613–8635. [CrossRef]